

# Organic carbon deposition flux on the North Chukchi Sea shelf based on $^{210}\text{Pb}$ radioactivity dating

LI Yiliang<sup>1,2</sup>, YU Wen<sup>1,2\*</sup>, HE Jianhua<sup>1,2</sup> & SU Jian<sup>1,3</sup>

<sup>1</sup> Key Laboratory of Global Change and Marine-Atmosphere Chemistry, State Oceanic Administration(SOA), Xiamen 361005, China;

<sup>2</sup> Third Institute of Oceanography, SOA, Xiamen 361005, China;

<sup>3</sup> Department of Engineering Physics, Tsinghua University, Beijing 100084, China

Received 21 August 2012; accepted 6 November 2012

**Abstract** Deposition of organic carbon forms the final net effect of the ocean carbon sink at a certain time scale. Organic carbon deposition on the Arctic shelves plays a particularly important role in the global carbon cycle because of the broad shelf area and rich nutrient concentration. To determine the organic carbon deposition flux at the northern margin of the Chukchi Sea shelf, the  $^{210}\text{Pb}$  dating method was used to analyze the age and deposition rate of sediment samples from station R17 of the third Chinese National Arctic Research Expedition. The results showed that the deposition rate was  $0.6 \text{ mm}\cdot\text{a}^{-1}$ , the apparent deposition mass flux was  $0.72 \text{ kg}\cdot\text{m}^{-2}\cdot\text{a}^{-1}$ , and the organic carbon deposition flux was  $517 \text{ mmol C}\cdot\text{m}^{-2}\cdot\text{a}^{-1}$ . It was estimated that at least 16% of the export organic carbon flux out of the euphotic zone was transferred and chronically buried into the sediment, a value which was much higher than the average ratio (~10%) for low- to mid-latitude regions, indicating a highly effective carbon sink at the northern margin of the Chukchi Sea shelf. With the decrease of sea ice coverage caused by warming in the Arctic Ocean, it could be inferred that the Arctic shelves will play an increasingly important role in the global carbon cycle.

**Keywords** organic carbon deposition,  $^{210}\text{Pb}$  dating, Chukchi Sea shelf

**Citation:** Li Y L, Yu W, He J H, et al. Organic carbon deposition flux on the North Chukchi Sea shelf based on  $^{210}\text{Pb}$  radioactivity dating. *Adv Polar Sci*, 2012, 23:231-236, doi: 10.3724/SP.J.1085.2012.00231

## 0 Introduction

The Arctic Ocean has a high potential for carbon sequestration, therefore the carbon cycle in the Arctic Ocean is one of the central issues in global climate change. After entering seawater via air-sea exchange, carbon dioxide is transformed into particulate organic carbon (POC) by the biological pump, and subsequently transferred from surface water to deep water. Most of the POC is remineralized by bacterial decomposition, will subsequently return to the atmosphere, and will not contribute to the sequestration of atmospheric carbon. Only a small amount of POC is buried in sediment and will contribute to the net effect of the carbon sink over long time scales. Marine organic carbon deposition flux is therefore very important in the study of

the Arctic Ocean carbon cycle<sup>[1]</sup>. Because of abundant continental input and high biological productivity, the organic carbon deposition flux in sea shelf regions can be tens of times higher than in the open ocean, and as a consequence approximately 80% of organic carbon deposition occurs in shelf areas<sup>[2]</sup>. Approximately one quarter of the global continental shelf area is in the Arctic Ocean, and as a result organic carbon deposition in this region plays a crucial role in the global carbon cycle<sup>[3]</sup>.

The Chukchi Sea is one of the Arctic marginal seas, located between Eurasia and North America, and adjacent to the Beaufort Sea, the East Siberian Sea, the central Arctic Basin, and Bering Strait. The area of the Chukchi Sea is  $620\,000 \text{ km}^2$ , and it has an average depth of 77 m with a shelf/slope ratio of approximately 7:1<sup>[4]</sup>. Unlike other Arctic marginal sea shelves, organic carbon deposition on the Chukchi Sea shelf results mainly from the biological pump process rather than continental input, which is an advantage

\* Corresponding author (email: yuwen2001@gmail.com)

for research on the efficiency of the marine biological pump. To date, studies on organic carbon deposition flux in the Arctic Ocean have focused on the Laptev, Kara, Barents, and Beaufort Seas<sup>[5-8]</sup>, and fewer data have been obtained from the East Siberian Sea, the Chukchi Sea, and the central Arctic Basin. Therefore, research on the organic carbon deposition flux in the Chukchi Sea is important and significant. In China, research on this process began with the first Chinese National Arctic Research Expedition (the 1st CHINARE-Arctic) in 1999. Yang et al.<sup>[5]</sup> analyzed one sediment core sampled from the west of the Chukchi Sea shelf, and found the organic carbon deposition rate in this region to be 358 mmol C·m<sup>-2</sup>·a<sup>-1</sup>, indicating that the Chukchi Sea has a high efficiency in organic carbon burial. However, there are few other domestic research results available on organic carbon deposition rates in the Chukchi Sea.

During the third Chinese National Arctic Research Expedition (the 3rd CHINARE-Arctic) in the International Polar Year 2008—2009 (July 11—Sept 24, 2008), a sediment core the station R17 was collected with a gravity corer from the station R17, the northern margin of the Chukchi Sea shelf (75°00.09' N, 168°08.73' W, bottom depth 163 m) (Figure 1). In this study, the organic carbon deposition rate at the northern margin of the Chukchi Sea shelf was determined using the <sup>210</sup>Pb dating technique. The results were compared with the POC flux from the euphotic zone, measured during the same cruise, and the organic carbon burial efficiency of the region was estimated.

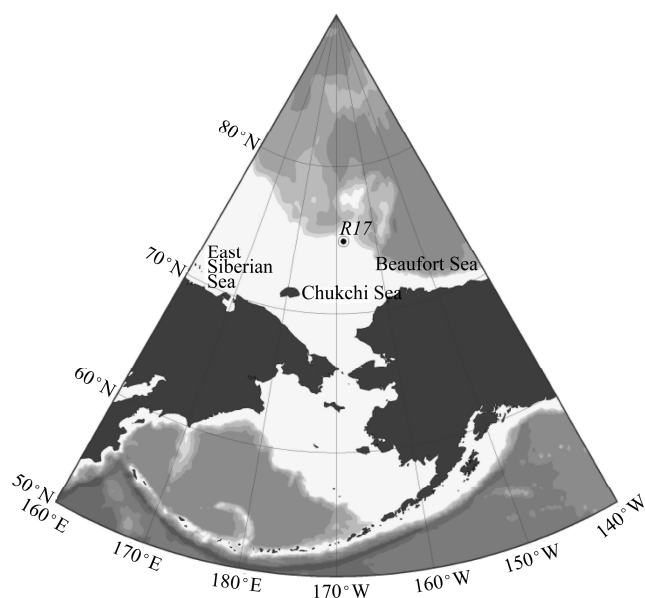


Figure 1 Sampling site.

## 1 Methods

### 1.1 The theory of the <sup>210</sup>Pb dating method

For the calculation of the organic carbon deposition rate, the age of the sediment core should be determined first.

Using the value of the organic carbon concentration in the surface sediment, the organic carbon deposition rate can then be calculated. With a half-life of 22.260 a, <sup>210</sup>Pb is one of the radionuclides in the uranium decay series, decayed from <sup>226</sup>Ra's gaseous state daughter, <sup>222</sup>Rn (Figure 2). After a short time (~10 d) in the atmosphere, <sup>210</sup>Pb falls on the sea surface in dry and wet precipitation, and later deposits into the sediment, resulting in an excess of <sup>210</sup>Pb relative to <sup>226</sup>Ra. The extent of <sup>210</sup>Pb excess can be used to calculate the age of sediment core slices, at a time scale of ~100 a.

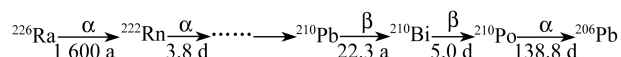


Figure 2 Decay chain of <sup>210</sup>Pb.

### 1.2 Sampling and pretreatment

A geological winch (10 000 m, Dynacon, USA) and a large-caliber gravity sampler (DDC-2, Institute of Oceanographic Instrumentation, Shandong Academy of Sciences, China) were used for sediment core sampling. The screened pipe was made of PVC, with an inner diameter of 116 mm. The sediment core was sealed at both ends and stored in an upright position in a 4°C refrigeration room, and cut into 1 cm slices after returning to the land-based laboratory. The wet weight of the slices was measured with an analytical balance. The slices were dried to constant weight at a temperature of 50°C, and ground until homogeneous. The sediment core used in this study was 47 cm long, with a diameter of 11 cm. The upper 22.5 cm of the core was composed mainly of light gray clay, with a sticky consistency. The lower part of the core consisted mainly of brown, yellow, and grayish-yellow clay, with a high degree of oxidation and stickiness. At the bottom there were a few plant roots, but no shells or foraminifer were found in the core sample.

### 1.3 Concentration, purification, and determination of <sup>210</sup>Pb

Eight slices from the upper 15 cm of the core were selected for the measurement of <sup>210</sup>Pb. Dry samples weighing 2 g were taken from each slice, ground, and placed into a 250 ml beaker, 0.6 dpm of <sup>209</sup>Po tracer and 25 ml of concentrated nitric acid (HNO<sub>3</sub>) were then added to the beaker. The mixture was evaporated to dryness in a water bath then 10 ml of concentrated HNO<sub>3</sub> was added into the beaker before a second evaporation to dryness in the water bath. Next, 15 ml of 6 M hydrochloric acid (HCl) was added to the beaker and heated for 20 min. The solution and residue were transferred into an organic glass centrifuge tube with 10 ml of 1 M HCl for a 3 min centrifugation. The supernatant was transferred into a 150 ml beaker, and the residue was rinsed twice with 2 M HCl before a second centrifugation. The supernatants were combined and 5 g of hydroxylamine hydrochloride was added. After adjusting the pH to 2, the solution was placed onto a thermostatic magnetic

stirrer, with the temperature set at  $85^\circ\text{C}$ . After 4 h of stirring,  $^{210}\text{Po}$  deposited onto the silver plate in the organic glass device. The silver plate was rinsed with deionized water and absolute ethyl alcohol, dried at room temperature, and  $^{209}\text{Po}$  and  $^{210}\text{Po}$  were detected with a low background alpha spectrometer (Canberra 7200-08, USA) until the counting error was  $<3\%$ .

#### 1.4 Organic carbon concentration analysis

Five hundred mg of dried sample was weighed, placed into a glass centrifuge tube, and sufficient 1 M HCl added to cover the sample. The tube was placed into an ultrasonic bath for 10 min, and then centrifuged. The supernatant was discarded and 5 ml of deionized water was added to the residue, which was then oscillated for 5 min. To get rid of leftover HCl, the above procedure was repeated twice. The sample was dried in a  $50^\circ\text{C}$  oven, and analyzed for organic carbon concentration with a total organic carbon analyzer (TOC-VCPH, SSM-5000A, Shimadzu, Japan) at a working temperature of  $900^\circ\text{C}$ .

#### 1.5 Sedimentation rate determination

The radioactivity of excess  $^{210}\text{Pb}$  ( $^{210}\text{Pb}_{\text{ex}}$ ) in the sediment core decays according to the following law:

$$A_h = A_0 e^{-\lambda t} \quad (1)$$

where  $A_h$  and  $A_0$  represent the  $^{210}\text{Pb}_{\text{ex}}$  radioactivity at the compaction adjusting depth  $h$  (cm) and at the sediment surface ( $h = 0$ ), respectively;  $\lambda$  is the decay constant of  $^{210}\text{Pb}$  ( $3.11 \times 10^{-2} \text{ a}^{-1}$ ), and  $t$  is the age (a) of the sediment where depth is  $h$ . Therefore,

$$\ln A_h = \ln A_0 - \lambda t \quad (2)$$

The age of the sediment is:

$$t = \frac{\ln(A_0 / A_h)}{\lambda} \quad (3)$$

When the sedimentation rate is constant, and  $s$  is the sedimentation rate (cm/a), i.e.,  $t = h/s$ , then

$$\ln A_h = \ln A_0 - \lambda h/s \quad (4)$$

There is a linear relationship between  $\ln A_h$  and  $h$ , with a slope of  $-(\lambda/s)$ . If  $\ln A_h$  is plotted against  $h$ , and the slope is  $a$ , the sedimentation rate is:

$$s = -\frac{\lambda}{a} \quad (5)$$

#### 1.6 Apparent deposition mass flux and organic carbon deposition rate calculation

There are two methods used to work out the  $^{210}\text{Pb}$  background radioactivity to calculate the excess  $^{210}\text{Pb}$  radioactivity, the direct approach and the indirect approach. The direct approach determines the background  $^{210}\text{Pb}$  radioactivity by measuring the radioactivity of  $^{226}\text{Ra}$  in the sample, assuming that  $^{226}\text{Ra}$  and  $^{210}\text{Pb}$  are in equilibrium. The indirect approach determines the background  $^{210}\text{Pb}$  radioactivity as the average  $^{210}\text{Pb}$  radioactivity in the background layer, where it tends to be constant. The direct approach is more accurate but the indirect approach is more applicable and

convenient. In this study we used the indirect approach.

The sedimentation rate calculated with Equation (5) was in  $\text{cm}\cdot\text{a}^{-1}$ . Given that compaction adjusting standard densities varies a lot across different studies, it is not easy to compare the sedimentation rate results. The apparent deposition mass flux, which reflects the nature of deposition and eliminates the effect of different compaction adjusting standard densities, is a more suitable parameter for comparing the results of different studies.

The apparent deposition mass flux is based on the accumulated mass depth  $m$  ( $\text{kg}\cdot\text{m}^{-2}$ ):

$$m = \sum_i (1-j) r_D \Delta x \quad (6)$$

where  $\varphi$  is the porosity of the sediment sample,  $r_D$  is the density of the dry sediment ( $\text{g}\cdot\text{cm}^{-3}$ ), taken to be  $2.5 \text{ g}\cdot\text{cm}^{-3}$ [6], and  $\Delta x$  is the thickness of the sliced sample.

The porosity of the sediment is defined as:

$$j = (W - D) / BV \quad (7)$$

where  $W$  and  $D$  are the wet weight (g) and dry weight (g) of the sliced sample, respectively, and  $BV$  is the bulk volume of the sliced sample, which can be defined by the following equation:

$$BV = W + [(1/r_D) - 1]D \quad (8)$$

Where  $r_D$  is the density of the dry sediment sample ( $\text{g}\cdot\text{cm}^{-3}$ ), taken to be  $2.5 \text{ g}\cdot\text{cm}^{-3}$ . The approximate expression of  $\varphi$  is then:

$$j = 1/[1/(2.5 \times \text{H}_2\text{O}\%) + 0.6] \quad (9)$$

Assuming the apparent deposition mass flux is constant, the profile of  $^{210}\text{Pb}_{\text{ex}}$  radioactivity is in accordance with the following equation:

$$\ln A_m = \ln A_0 - I r/m \quad (10)$$

where  $A_m$  and  $A_0$  are the  $^{210}\text{Pb}_{\text{ex}}$  radioactivity ( $\text{dpm}\cdot\text{g}^{-1}$ ) at accumulated mass depth  $m$  (cm) and at the surface, respectively, and  $r$  is the apparent deposition mass flux ( $\text{kg}\cdot\text{m}^{-2}\cdot\text{a}^{-1}$ ), which can be calculated by the linear fitting slope  $b$  of  $\ln A_m$  to  $m$ :

$$r = -\frac{I}{b} \quad (11)$$

Based on the apparent deposition mass flux  $r$  and the organic carbon concentration in the surface sediment OC% ( $\text{mmol C}\cdot\text{kg}^{-1}$ ), the organic carbon deposition rate  $F_{\text{OC}}$  ( $\text{mmol C}\cdot\text{m}^{-2}\cdot\text{a}^{-1}$ ) can be calculated as:

$$F_{\text{OC}} = r \times \text{OC}\% \quad (12)$$

## 2 Results and discussion

### 2.1 Radioactivity of $^{210}\text{Pb}$ , water content, and organic carbon concentration

The radioactivity of  $^{210}\text{Pb}$  ( $A^{210}\text{Pb}$ ) and excess  $^{210}\text{Pb}$  ( $A^{210}\text{Pb}_{\text{ex}}$ ), water content ( $\text{H}_2\text{O}\%$ ), and organic carbon concentration (OC%) are listed in Table 1, and the profile of these parameters is shown in Figure 3. The background radioactivity used for calculating the  $^{210}\text{Pb}_{\text{ex}}$  radioactivity was the average of  $^{210}\text{Pb}$  radioactivity for the lower four slices listed in Table 1 ( $1.064 \text{ dpm}\cdot\text{g}^{-1}$ ). The  $^{210}\text{Pb}$  radioactivity in the surface sediment was  $1.335 \text{ dpm}\cdot\text{g}^{-1}$ , which is

lower than the typical value ( $2\text{--}3 \text{ dpm}\cdot\text{g}^{-1}$ ) for low latitude shelves, probably a consequence of the unique geographical location and natural conditions of the sampling site. The broad permafrost zone around the Arctic Ocean prevents  $^{222}\text{Rn}$  from escaping and therefore reduces the source of its daughter  $^{210}\text{Pb}$ . Furthermore, the wide distribution of sea ice at the northern margin of Chukchi Sea cuts off the transferring channel for  $^{210}\text{Pb}$ . A combination of these factors may explain the lower level of  $^{210}\text{Pb}$  in the surface sediment in this region.

The organic carbon concentration gradually decreased with depth in the upper slices, indicating the degradation of organic carbon. There was an abnormally high value in the 5–6 cm slice, possibly as a result of an algae outbreak or man-induced event in the corresponding period ( $\sim 1910\text{--}1926$ , from the sedimentation rate deduced below), which requires further analysis, such as chemical and grading composition analysis.

**Table 1** Analysis results of  $^{210}\text{Pb}$  radioactivity ( $A^{210}\text{Pb}$  and  $A^{210}\text{Pb}_{\text{ex}}$ ), water content ( $\text{H}_2\text{O}\%$ ), and organic carbon content ( $\text{OC}\%$ )

Depth/cm	$A^{210}\text{Pb}/(\text{dpm}\cdot\text{g}^{-1})$	$A^{210}\text{Pb}_{\text{ex}}/(\text{dpm}\cdot\text{g}^{-1})$	$\text{H}_2\text{O}\%$	$\text{OC}\%$
0–1	$1.335 \pm 0.119$	$0.271 \pm 0.119$	28.8	0.857 9
1–2	$1.288 \pm 0.100$	$0.224 \pm 0.100$	29.1	0.832 0
2–3	$1.188 \pm 0.097$	$0.124 \pm 0.097$	27.3	0.822 8
3–4	$1.118 \pm 0.095$	$0.054 \pm 0.095$	29.1	0.796 7
5–6	$1.052 \pm 0.095$	$-0.012 \pm 0.095$	29.9	0.967 3
6–7	$1.061 \pm 0.098$	$-0.003 \pm 0.098$	28.6	0.803 8
12–13	$1.074 \pm 0.102$	$0.010 \pm 0.102$	27.1	0.846 8
14–15	$1.069 \pm 0.094$	$0.005 \pm 0.094$	27.0	0.860 4

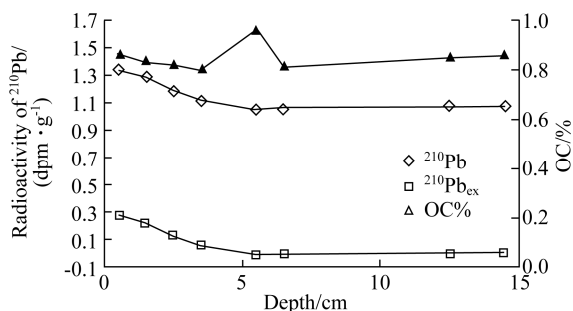


**Figure 3** Profile of  $^{210}\text{Pb}$  radioactivity and POC content.

## 2.2 Sedimentation rate

Figure 4 plots the natural logarithm values of  $A^{210}\text{Pb}$  and  $A^{210}\text{Pb}_{\text{ex}}$  against compaction adjusting depth  $h$ . This shows that the profile of  $A^{210}\text{Pb}$  has a typical two-stage distribution, where the natural logarithm values of  $A^{210}\text{Pb}$  decreased linearly in the decay layer ( $h = 0\text{--}5 \text{ cm}$ ) and stayed constant in the background layer ( $h > 5 \text{ cm}$ ). There was no mixed layer in the sediment core, which was consistent with a relative lack of disturbance factors (e.g., human ac-

tivities or fluvial abrasion of rivers) because the sampling site was distant from the continent.

A linear fitting process was applied to the data from the decay layer, and a linear equation of  $y = -0.54x - 0.8689$  was derived with  $R^2 = 0.9362$  indicating a good linear fit. The linear equation derived above was extrapolated to the surface, and an  $A^{210}\text{Pb}_{\text{ex}}$  initial content of  $0.419 \text{ dpm}\cdot\text{g}^{-1}$  was obtained. The sedimentation rate was  $0.6 \text{ mm}\cdot\text{a}^{-1}$ , calculated from Equation (5) and the slope of the linear fit. This value was slightly lower than the results obtained from the western Chukchi Sea shelf by Yang et al.<sup>[5]</sup> ( $0.7 \text{ mm}\cdot\text{a}^{-1}$ ), and from the mid Chukchi Sea by Huh et al.<sup>[7]</sup> ( $0.8 \text{ mm}\cdot\text{a}^{-1}$ ), possibly because of less continental input (e.g., river inflow and coast erosion) at the sampling site in this study. On the other hand, the sedimentation rate calculated in this study was slightly higher than the value of  $0.43 \text{ mm}\cdot\text{a}^{-1}$ <sup>[8]</sup> obtained from the northern margin of the Laptev Sea shelf, possibly because of the higher biological productivity over the Chukchi Sea shelf<sup>[9]</sup>.

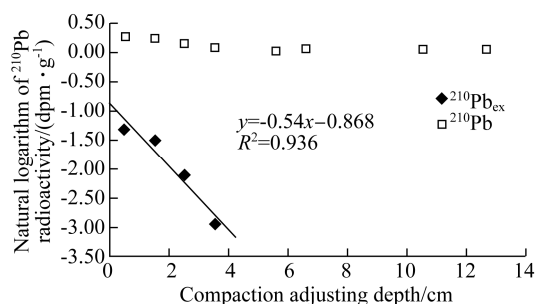


**Figure 4** Relationship of the natural logarithm of  $^{210}\text{Pb}$  radioactivity to compaction adjusting depth.

## 2.3 Apparent deposition mass flux

The calculated results of porosity ( $\phi$ ) and accumulated mass depth ( $m$ ) are listed in Table 2. Figure 5 plots the natural logarithm value of the  $^{210}\text{Pb}_{\text{ex}}$  radioactivity against accumulated mass depth. The apparent deposition mass flux calculated using the slope of the linear fit and Equation (11) was  $0.72 \text{ kg}\cdot\text{m}^{-2}\cdot\text{a}^{-1}$ , which was in the range of  $0.31\text{--}3.24 \text{ kg}\cdot\text{m}^{-2}\cdot\text{a}^{-1}$  reported by Baskaran and Naidu<sup>[9]</sup>, and close to the values of  $0.55 \text{ kg}\cdot\text{m}^{-2}\cdot\text{a}^{-1}$  calculated by Huh et al.<sup>[7]</sup> and  $1 \text{ kg}\cdot\text{m}^{-2}\cdot\text{a}^{-1}$  by Yang et al.<sup>[5]</sup>.

**Table 2** Porosity and accumulated mass depth

Depth/cm	$\phi$	$m/(\text{kg}\cdot\text{m}^{-2})$
0–1	0.50	6.2
1–2	0.51	18.6
2–3	0.48	31.2
3–4	0.51	43.8
5–6	0.52	69.1
6–7	0.50	81.4
12–13	0.48	130.7
14–15	0.48	157.3

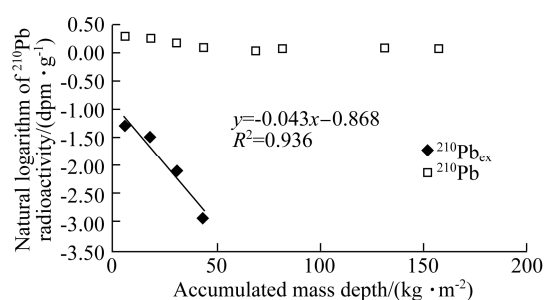


**Figure 5** Relationship of the natural logarithm of  $^{210}\text{Pb}$  radioactivity to accumulated mass depth.

## 2.4 Organic carbon deposition rate and comparison with POC export flux from the euphotic zone

Using the result of the apparent deposition mass flux obtained in Section 2.3 ( $0.72 \text{ kg} \cdot \text{m}^{-2} \cdot \text{a}^{-1}$ ) and the organic carbon concentration in the surface sediment (0.857 9%), the organic carbon deposition rate at the sampling site R17 was calculated to be  $517 \text{ mmol C} \cdot \text{m}^{-2} \cdot \text{a}^{-1}$ . This was lower than the result ( $3141 \text{ mmol C} \cdot \text{m}^{-2} \cdot \text{a}^{-1}$ ) obtained at the western Chukchi Sea shelf by Yang et al.<sup>[5]</sup>, but close to the result ( $358 \text{ mmol C} \cdot \text{m}^{-2} \cdot \text{a}^{-1}$ ) obtained at the northern margin of Laptev Sea shelf by Stein and Fahl<sup>[8]</sup>. The comparison between the results of this study and previous studies is summarized in Table 3.

Ideally, we should compare the organic carbon deposition rate calculated above to the annual POC export flux obtained by sediment traps to determine the efficiency of biological pump. However, it is difficult to deploy sediment traps in shallow and ice covered regions such as the Chukchi Sea shelf. Therefore, for this study, we estimated the annual POC export flux based on the POC export flux determined using  $^{234}\text{Th}$ - $^{238}\text{U}$  disequilibrium during the same research cruise (the 3rd CHINARE-Arctic). It should be noted that organic carbon could be remineralized during early diagenesis, which will influence the accuracy of the calculated results.

The Chukchi Sea is frozen for much of the year and there are only 3–4 months per year when the sea surface is not covered by sea ice. Stein and Macdonald found that plankton grew abundantly and organic carbon export occurred only on 60 days during this ice-free period<sup>[10]</sup>. Taking this finding into account, the average organic carbon deposition rate at the northern margin of Chukchi Sea shelf during summer was  $8.6 \text{ mmol C} \cdot \text{m}^{-2} \cdot \text{d}^{-1}$ . By comparing this result with POC export flux from the euphotic zone ( $29.5 \pm 23.0 \text{ mmol C} \cdot \text{m}^{-2} \cdot \text{d}^{-1}$ ) obtained during the 3rd CHINARE-Arctic<sup>[11]</sup>, at least 16% of the organic carbon transported to deep water by the biological pump was sealed in the sediment and kept stable for a long time. The ratio was 50% higher than that typically found for mid- and low-latitude regions (~10%), which supported the existence of a highly efficient organic sink effect on the Chukchi Sea shelf.

**Table 3** Research results of adjacent regions

Study region	$s$ /( $\text{mm} \cdot \text{a}^{-1}$ )	$r$ /( $\text{kg} \cdot \text{m}^{-2} \cdot \text{a}^{-1}$ )	$F_{\text{OC}}$ /( $\text{mmol C} \cdot \text{m}^{-2} \cdot \text{a}^{-1}$ )	Reference
North margin of Laptev Sea shelf	0.43	NR	358	[8]
Western Chukchi Sea shelf	0.7	1	3141	[5]
Chukchi Sea slope	0.89	0.55	NR	[7]
North margin of Chukchi Sea shelf	0.6	0.72	517	This study

Notes: NR—not reported,  $s$ —sedimentation rate,  $r$ —apparent deposition mass flux,  $F_{\text{OC}}$ —organic carbon depositional flux.

## 3 Conclusion

In this study, the organic carbon deposition rate at the northern margin of the Chukchi Sea shelf was estimated using the  $^{210}\text{Pb}$  dating method. The radioactivity of  $^{210}\text{Pb}$  in the surface sediment sample was  $1.335 \text{ dpm} \cdot \text{g}^{-1}$ , lower than the typical value (2–3  $\text{dpm} \cdot \text{g}^{-1}$ ) for low latitude shelves, mainly because of the extensive sea-ice coverage and broad permafrost zone around the study region. The sedimentation rate calculated using  $^{210}\text{Pb}$  dating was  $0.6 \text{ mm} \cdot \text{a}^{-1}$ , the apparent deposition mass flux was  $0.72 \text{ kg} \cdot \text{m}^{-2} \cdot \text{a}^{-1}$ , and the organic carbon depositional flux was  $517 \text{ mmol C} \cdot \text{m}^{-2} \cdot \text{a}^{-1}$ . These values were all lower than those obtained at the western Chukchi Sea shelf but close to the results obtained at the northern margin of the Laptev Sea shelf. Comparison with the POC export flux from the euphotic zone, measured during the same expedition, showed that at least 16% of the organic carbon exported from the euphotic zone was sealed in the sediment. This was much higher than the value (~10%) for mid- and low-latitude sea shelves, indicating that the carbon sink effect is highly efficient at the northern margin of the Chukchi Sea shelf.

**Acknowledgments** This study was supported by the Scientific Research Foundation of the Third Institute of Oceanography, SOA (Grant nos. 2011024 and 2011025), and the Marine Science Youth Fund of SOA (Grant no. 2012107). Samples used in this study were provided by the Polar Sediment Repository of the Polar Research Institute of China (PRIC). Samples information and data were issued by the Resource-sharing Platform of Polar Samples (<http://birds.chinare.org.cn>) maintained by PRIC and Chinese National Arctic & Antarctic Data Center (CN-NADC). Data were issued by the Data-sharing Platform of Polar Science (<http://www.chinare.org.cn>) maintained by PRIC.

## References

- Berger W H, Smetacek V S, Wefer G. Productivity of the Ocean: Present and Past. Chichester: John Wiley & Sons, 1989: 471.
- Hedges J I, Keil R G. Sedimentary organic matter preservation: an assessment and speculative synthesis. *Marine Chemistry*, 1995, 49(2-3): 81-115.
- Chen J F, Zhang H S, Jin H Y, et al. Accumulation of sedimentary organic carbon in the Arctic shelves and its significance on global carbon budget.

- Chinese Journal of Polar Research, 2004, 16(3): 193-201.
- 4 Stein R, Macdonald R W. The Organic Carbon Cycle in the Arctic Ocean. New York: Springer, 2004: 1-5.
  - 5 Yang W F, Chen M, Liu G S, et al. The distribution of radionuclides at Chukchi Sea shelf sediment and its tracing of sedimentary environment. *Advances in Natural Science*, 2002, 12(5): 515-518 (in Chinese).
  - 6 Hermanson M H.  $^{210}\text{Pb}$  and  $^{137}\text{Cs}$  chronology of sediments from small, shallow Arctic lakes. *Geochem. Cosmochem. Acta*, 1990, 54(5): 1443-1451.
  - 7 Huh C A, Pisias N G, Kelley J M, et al. Natural radionuclides and plutonium in sediments from the western Arctic Ocean: sedimentation rates and pathways of radionuclides. *Deep Sea Research Part II: Topical Studies in Oceanography*, 1997, 44(8): 1725-1743.
  - 8 Stein R, Fahl K. Holocene accumulation of organic carbon at the Laptev Sea continental margin (Arctic Ocean): sources, pathways, and sinks. *Geo-Marine Letters*, 2000, 20(1): 27-36.
  - 9 Baskaran M, Naidu A S.  $^{210}\text{Pb}$ -derived chronology and the fluxes of  $^{210}\text{Pb}$  and  $^{137}\text{Cs}$  isotopes into continental shelf sediments, East Chukchi Sea, Alaskan Arctic. *Geochimica et Cosmochimica Acta*, 1995, 59(21): 4435-4448.
  - 10 Stein R, Macdonald R W. The Organic Carbon Cycle in the Arctic Ocean. New York: Springer, 2004: 1-5.
  - 11 Yu W, He J H, Li Y L, et al. Particulate organic carbon export fluxes and validation of steady state model of  $^{234}\text{Th}$  export in the Chukchi Sea. *Deep-Sea Research II*, 2012, 81-84: 63-71. doi:10.1016/j.dsr2.2012.03.003.